

Article

# Microstructure Evolution and Lifetime Extension Mechanism of Sn-Added Fe-Based Pre-Alloy Brazing Coating in Diamond Tools

Dashuang Liu <sup>1,2</sup>, Weimin Long <sup>2,\*</sup>, Mingfang Wu <sup>1,\*</sup>, Kai Qi <sup>1</sup> and Juan Pu <sup>1</sup>

<sup>1</sup> School of Material Science and Engineering, Jiangsu University of Science and Technology, Zhenjiang 212003, China; dslu@just.edu.cn (D.L.); qikai@just.edu.cn (K.Q.); wpjw01@126.com (J.P.)

<sup>2</sup> Zhengzhou Research Institute of Mechanical Engineering Co., Ltd., Zhengzhou 450001, China

\* Correspondence: brazelong@163.com (W.L.); wumingfang@just.edu.cn (M.W.);  
Tel.: +86-511-844-01184 (M.W.)

Received: 18 March 2019; Accepted: 28 May 2019; Published: 4 June 2019



**Abstract:** The effect of Sn content added in pre-alloy powder on the microstructure, porosity, hardness and bending strength of hot pressing sintering of a diamond matrix was investigated. The results show that with the increase of Sn content in the pre-alloy powder, a reduction in grain size and porosity as well as an increase in hardness is observed. As a result of the reduction in porosity, the flexural strength increases with the increase in the Sn content in the pre-alloy powder. However, with the increase of Sn content, the bending strength decreases owing to the formation of Cu<sub>5,6</sub>Sn in the matrix. The properties of the diamond matrix are improved, and the lifetime of the diamond matrix is prolonged when the Sn content is 4 wt.%.

**Keywords:** pre-alloy powder; Sn content; organization structure; mechanical property

## 1. Introduction

Diamond has good wear resistance, stable physical and chemical properties, as well as good corrosion resistance, radiation resistance and thermal conductivity. Diamond is widely used in cutting tools, particularly for precision machining [1,2]. However, diamonds in nature are not easy to form; the output is small and the price is too expensive. At present, synthetic diamonds are widely used in geological drilling and for the cutting of brittle and hard materials.

The main manufacturing methods of diamond tools are sintering, welding and electroplating, excimer laser ablation and thermal spraying [3–6]. Single-layer diamond tools are a common standard in the diamond tool industry. In most cases they are produced by electroplating, whereas nickel is used as a deposited metal. As there is no joining process between the electroplated metal and the diamond grit, the diamond retention comes only from mechanical fixing by covering the diamonds over more than 50% of their diameter [4,5]. The active brazing of diamonds is a highly interesting alternative to electroplating [7]. Cutting tool performance is mainly characterized by material substrate, cutting edge geometry and coating [8]. Moreover, the surface topography of the different blades is evaluated to examine the impact of wear depending on the surface profile and the distribution of the diamonds in the blade's substrate [9]. The surface degradation of coatings is also addressed to describe the interaction of the coated surface and different sizes of graphite embedded in the lubricant's matrix [10].

Diamond tools are usually sintered by basal body, diamond and matrix powder. The cutter head is composed of diamond and matrix. Thus the properties of the diamond and matrix determine the quality of diamond tools. In diamond tools, diamond is a cutting element, but when determining whether the diamond can be fully and effectively utilized, it is the matrix that plays a decisive role. The matrix mainly has two functions; “package” diamond and diamond “match” wear. The performance

of the matrix depends largely on the material of the matrix. The matrix mainly consists of metal, resin and ceramics, and is widely used because of its excellent comprehensive performance [11–14]. The preparation and formulation design of matrix powder on the cutter head have become the focus of much research on the quality of diamond tools.

In the process of using diamond tools, the main failure form is diamond shedding, not grinding failure, resulting in a lot of waste [15]. The most effective way to improve the comprehensive performance and life of diamond tools is to increase the holding force of the matrix to diamond, and improve the tool performance in a variety of work materials [16]. Using Cu–Sn pre-alloyed powder as bonding agent, the sintering temperature is low, which not only avoids gravity segregation and low melting point material loss caused by mechanical mixing powder, but also improves the wettability of the alloy to diamond and ensures the bonding strength between the matrix alloy and diamond.

In order to solve the problem of lifetime, pre-alloyed powders were added to matrix powders instead of metal powders and sintered by hot pressing to form brazing bonds between the matrix powders and diamond particles [17]. Improving the quality of diamond particles can improve the performance of diamond tools and prolong their lifetime to a certain extent, but the cost of improving the quality of the diamond is too high, and is generally reserved only for high-end products. The method of improving the skeleton material can prolong the lifetime, but it will reduce the sharpness of diamond tools, and adjusting the skeleton material cannot improve the comprehensive performance. Nowadays, the application requirements are mainly met by changing the binder. The binder can improve the wettability of the matrix to diamond, and make brazing connections between the matrix and diamond. This method is a very effective way to improve the comprehensive performance and lifetime of diamond tools, instead of simply inserting diamond in a matrix [18–20]. When pre-alloyed powder is used as binder, not only can the matrix powder diffuse, but the matrix and diamond can also be joined by diffusion brazing, which enhances the bonding force [21].

There are three kinds of brazing for diamond tools; single layer brazing, diamond bit brazing and polycrystalline diamond compact bit (PDC) composite brazing. The brazing process is the metallurgical bonding of diamond, filler metal and metal matrix, to provide high bonding strength [22]. The use of pre-alloyed powder is an effective way to improve the comprehensive performance of diamond cutter heads. Active pre-alloyed powder can improve the lifetime of diamond tools. In this study, the effect of Sn content added in pre-alloy powder on the microstructure, porosity, hardness and bending strength of hot press sintered diamond matrix was investigated.

## 2. Experimental Material and Methods

### 2.1. Experimental Material

Material selected in the experiment included iron powder, copper powder, tin powder, zinc powder, nickel powder and self-made pre-alloy powder. The particle size was -200 mesh. Among them, the pre-alloyed powder was prepared by multistage tightly coupled atomization, and the composition ratio of pre-alloyed powder is shown in Table 1. Figure 1 shows SEM morphologies of the pre-alloyed powder. It shows that most of the powders are spherical.

**Table 1.** Composition ratio of pre-alloyed powder (wt.%).

Pre-Alloyed Powder	Composition Ratio (wt.%)
Cu	15–25
Zn	10–15
Sn	0–10
Ni	3–12
Fe	Balance

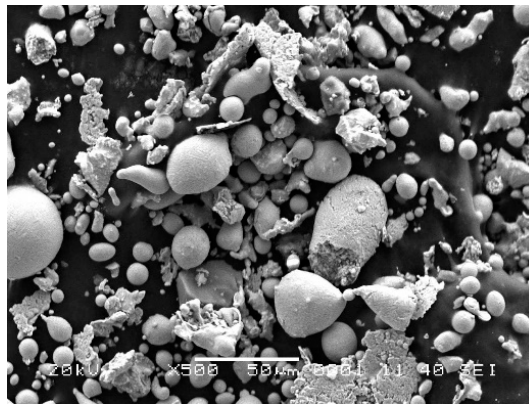


**Figure 1.** SEM morphologies of pre-alloyed powder.

### 2.2. Formulation Design of Matrix Powder on the Tool Head

This experiment mainly studied the effect of the Sn content in the pre-alloyed powder on the tissue and the performance of the blank matrix and cutter head. Six experimental formulas were formulated, which are 1#, 2#, 3#, 4#, 5# and 6#, with Sn contents of 0%, 2%, 4%, 6%, 8% and 10%, respectively.

### 2.3. Experimental Process

Several metal powders, such as Cu and Ni, are easy to oxidize at room temperature. Because of the existence of oxides, the graphitization of diamond will be aggravated and the surface of diamond will be strongly corroded, which leads to the aggravation of diamond breakage in the cutting process. Restoring equipments include gas making equipment and a restoring furnace. Moreover, the restoring agent is hydrogen or gas. During the sintering process, the gas is preperited to form a pore, resulting in the strength of the matrix and the tool head being reduced. Thus, it first needs to be restored. The die is needed as the carrier. There are two main points: (1) the compressive strength of the graphite should be over 40 Mpa and (2) graphite with low porosity must be selected with a density of less than 30%. This is mainly because the metal powder will enter into the micropores at the graphite surface, and the die will become brittle. Therefore, the density of the die should be above 1.6 g/cm<sup>3</sup>.

The material was proportioned according to the formula, weighed to requirement, and paraffin was added. The material was put in a three-dimensional mixer and taken out after an hour, then put into the graphite mold in the hot press sintering machine for sintering. In the sintering process (shown in Figure 2), the sintering temperature was 800 °C and the holding time was 60 s. After sintering, the sample size was 40 mm × 8 mm × 3.2 mm. The specific sintering process is shown in Figure 2.

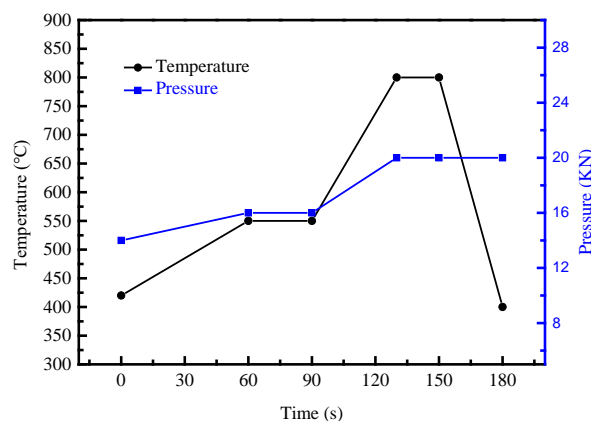


**Figure 2.** Sintering process of powders.

#### 2.4. Performance Testing Method

Archimedes' drainage method was used to measure the density of the sample [23]. The sample density was calculated according to formula  $\rho = m_{\text{air}} \cdot \rho_{\text{water}} / (m_{\text{air}} - m_{\text{water}})$ , where  $m_{\text{air}}$  is the weight of the samples in air,  $m_{\text{water}}$  is the weight of the sample in water and  $\rho_{\text{water}}$  is the density of water.

A Rockwell hardness tester (HRB) was used for the measurement of hardness of the samples in order to prevent cracking and other phenomena in the process of hardness testing. It is necessary to measure the HRB perpendicular to the pressing direction, and the reported values are an average of three data points. The three-point bending method on a universal material testing machine was used to measure the bending strength of the sintered samples. The loading direction was perpendicular to the pressing direction of the sample. The loading speed was 1 mm/min. The reported values are an average of three data points per sample.

A ZEISS optical microstructure (OM, Oberkochen, Germany) was used to observe the microstructure of sample. A JSM-6480 scanning electron microscope (SEM, JEOL, Tokyo, Japan) was used to observe the fracture morphology of the sample, and an XRD-6000 X-ray diffraction instrument (XRD, Shimadzu, Kyoto, Japan) was used to observe the tissue. X-ray diffraction (XRD) analysis was carried out with Cu-K $\alpha$  radiation and scanning angles ( $2\theta$ ) between  $10^\circ$  and  $90^\circ$ .

### 3. Results and Discussion

#### 3.1. Effect of Sn Content on the Microstructure Evolution

Figure 3 shows the microstructure of the matrix of sintered samples with different Sn contents. Figure 3a shows that the grain is coarse and the distribution of copper-based bonding phase is not uniform. Figure 3b–e show that the grains gradually become fine and the phase of copper-based bonding begins to distribute uniformly around the iron-based matrix. Therefore, the grain size grows finer with the increase of the Sn content.

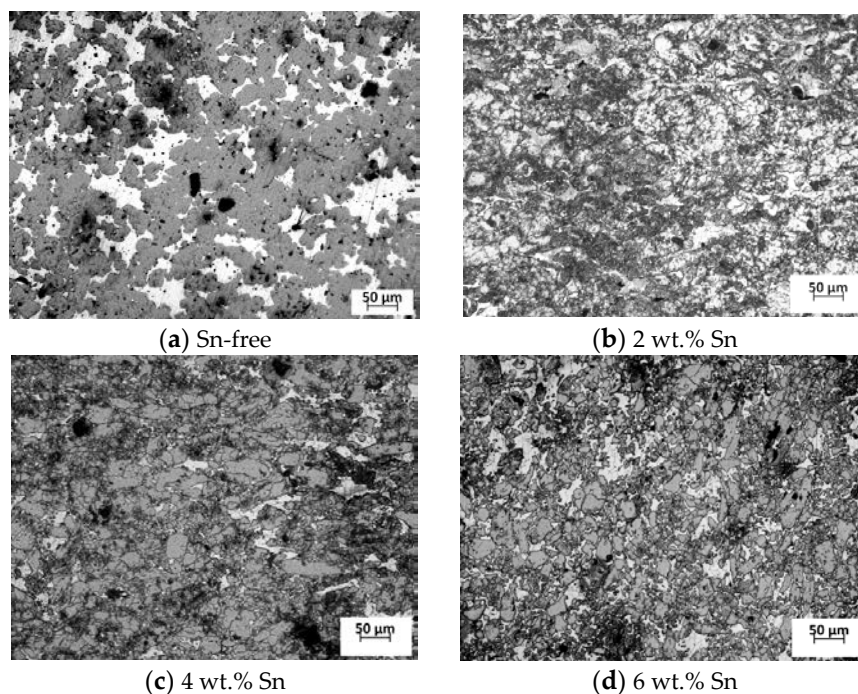
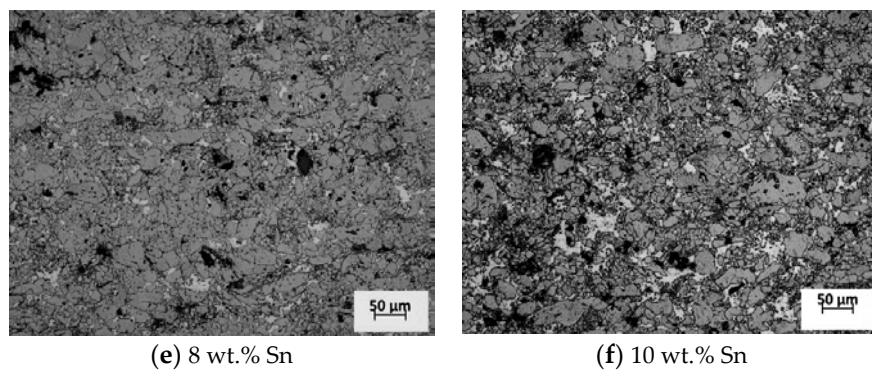
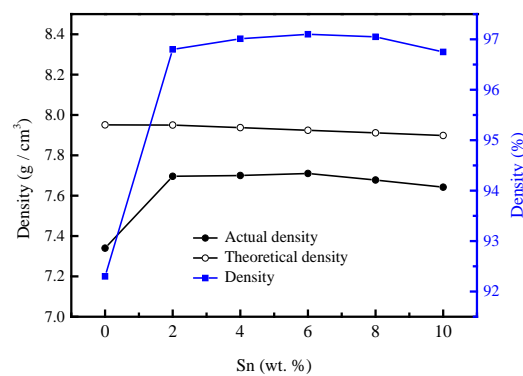


Figure 3. Cont.



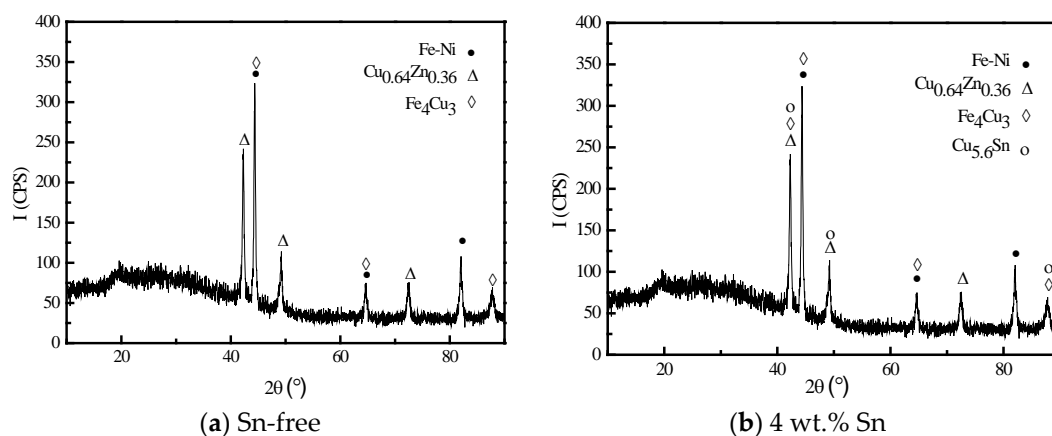
**Figure 3.** Microstructures of matrix of sintered samples with different Sn contents.

Figure 4 shows the effect of Sn content on the density of the matrix. It can be seen that the porosity decreases and the density of samples increases with the increase in Sn content in the powder. Moreover, when the Sn content is increased up to 2 wt.%, the sintering density of powder is increased greatly. With the increase of the low melting point element Sn, the liquid phase is increased. As reported in [24], the existence of the liquid phase is beneficial to the increase of the sintering density. Thus, the powder is compressed and the sintering density is increased owing to the increase of the viscous flow of the liquid phase and the capillary force formed by the liquid phase in the pores.



**Figure 4.** Density of the matrix of sintered samples with different Sn contents.

Figure 5 shows the XRD analysis results of the matrix phase of samples with different Sn contents. The phases in the Sn-free sample are mainly composed of  $\text{Fe}_4\text{Cu}_3$ ,  $\text{Cu}_{0.64}\text{Zn}_{0.36}$  and FeNi (see Figure 5a). With the increase of the Sn content, the new phase  $\text{Cu}_{5.6}\text{Sn}$  is observed (see Figure 5b). Therefore, the addition of Sn leads to the formation of  $\text{Cu}_{5.6}\text{Sn}$ . Similar results have been found in Cu–Sn alloy [25].



**Figure 5.** XRD analysis results of the matrix phase of samples with different Sn contents.

### 3.2. Lifetime Extension Mechanism of Sn-Added Fe-Based Pre-Alloy Brazing Coating in Diamond Tools

#### 3.2.1. Effect of Sn Content on Hardness of Matrix

Sintering temperature and holding time are the two most important factors in the sintering process, playing a decisive role in atomic diffusion. With an increase in sintering time, the density, hardness and bending strength of the matrix first increase and then decrease [26]. Under the condition that the parameters of the sintering process remain unchanged, the hardness of the matrix is only related to the chemical composition. Figure 6 shows the hardness of the matrix for different Sn contents in the powder. When no Sn is present in the powder, the hardness is only 80 HRB, and with the increase of Sn content from 0% to 10%, the hardness increases from 80 to 100 HRB. There are three main reasons for this. On the one hand, the pre-alloyed powder has higher hardness than the framework material, and with the increase of Sn content, the proportion of pre-alloyed powder increases and the hardness increases. On the other hand, with the increase of low melting point material, more liquid phase appears in the sintering process and the liquid phase produced fills the gaps among the powder particles. The material then shrinks through the capillary force appearing in the liquid phase, thus the density and the hardness increase with the increase in Sn content in the powder. The authors of [27] reported similar results, namely that the strength of the pre-alloy matrix is improved owing to the addition of low melting point elements. Secondly, by comparing with Figure 3, it can be seen that the grain size of the matrix sample becomes finer with Sn addition, which explains the observed hardness increase with Sn addition to the powder.

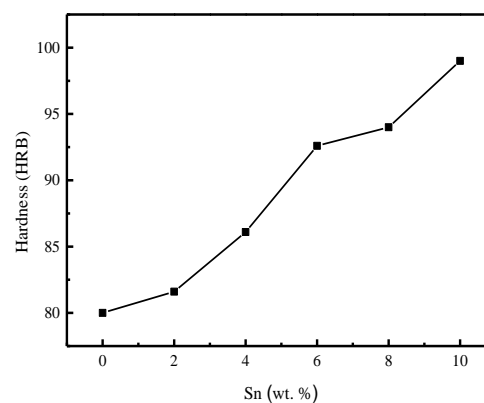


**Figure 6.** The hardness of the matrix of sintered samples with different Sn contents.

For powder metallurgy materials, the hardness, bending strength and other mechanical properties are mainly affected by density. With the increase of density, the mechanical properties such as hardness and bending strength also increase [28]. When the Sn content is between 2 and 6 wt.%, the hardness increases rapidly. Figure 4 shows that when the Sn content is between 2 and 6 wt.%, there is no significant change in the density of the samples. This is mainly because more liquid phase has been produced. After filling the gap between the powder, there is still more liquid phase, phenomenon of running materials gradually appears, which will lead to a slower increase in density. As the density of the matrix increases, the hardness also increases. With the increase of Sn content, more  $\text{Cu}_{5,6}\text{Sn}$  brittle and hard phases will be formed, resulting in an increase in hardness. When the content of Sn increases again, the density decreases slightly, but the change is not significant mainly because the phenomenon of running materials starts to appear (low melting point material flows out from the gap of the mold). However, with the formation of more  $\text{Cu}_{5,6}\text{Sn}$  brittle and hard phases, the hardness will still increase.

#### 3.2.2. Effect of Sn Content on Shearing Strength and Bending Strength of Matrix

Figure 7 shows the shearing strength and bending strength of matrix with different Sn additions. It can be seen that the shearing strength is 350 MPa in the Sn-free matrix. With the increase of Sn

content, the shearing strength is increased. When Sn content is increased up to 4 wt.%, the shear strength decreases. The increase of shearing strength is related to the increase of the density due to the Sn addition. However, when the Sn content exceeds 4 wt.%, the deterioration of shearing strength contributes to the formation of the brittle phase. The bending strength of the matrix shows a similar trend, where the bending strength increases first with the increase in Sn content reaching a maximum value of 612 MPa for 4 wt.% Sn. Beyond 4 wt.% Sn in the powder, the bending strength decreases. There are three main reasons for the observed trend. Firstly, in the sintering process, the material with a low melting point melts first to form a liquid phase, which improves the compressibility.

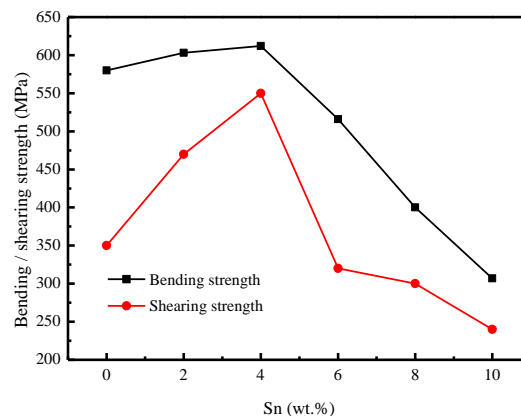


**Figure 7.** Bending strength of matrix of sintered samples with different Sn contents.

Through the capillary force appearing in the liquid phase, the material shrinks and achieves densification, thus enhancing the bending strength; on the other hand, the pre-alloyed powder has higher hardness than the framework material. With the increase of the whole proportion of pre-alloyed powder, the hardness of matrix increases. The hardness is related to the strength of the material, so the bending strength of the matrix is improved to some extent. Secondly, Figure 3 shows that with the increase of Sn content the grain size of the matrix becomes smaller and the mechanical properties are improved, so that the bending strength is improved. The stability of diamond tools in the grinding process is improved, and the service life of diamond tools is prolonged [29]. When Sn content exceeds 4%, it can be found that the bending strength decreases with the increase of Sn content. The decrease of bending strength is mainly due to the excessive content of Sn and the formation of excessive  $\text{Cu}_{5,6}\text{Sn}$  compounds, which decreases the toughness and increases the brittleness of the matrix. Although the grain size decreases and the bending strength increases to a certain extent, due to the formation of too many  $\text{Cu}_{5,6}\text{Sn}$  compounds the bending strength of the matrix decreases.

Figure 8 shows the SEM fracture diagram of the sample after three-point bending—the Sn-free sample shows a brittle-ductile mixed fracture, and a certain number of dimples exist at the fracture [30]. It can be seen that there are more dimples at the fracture of samples with the Sn content increased up to 4 wt.%, and the fracture mode is ductile. The samples with the Sn content exceeding 4 wt.% exhibit mainly brittle fracture.

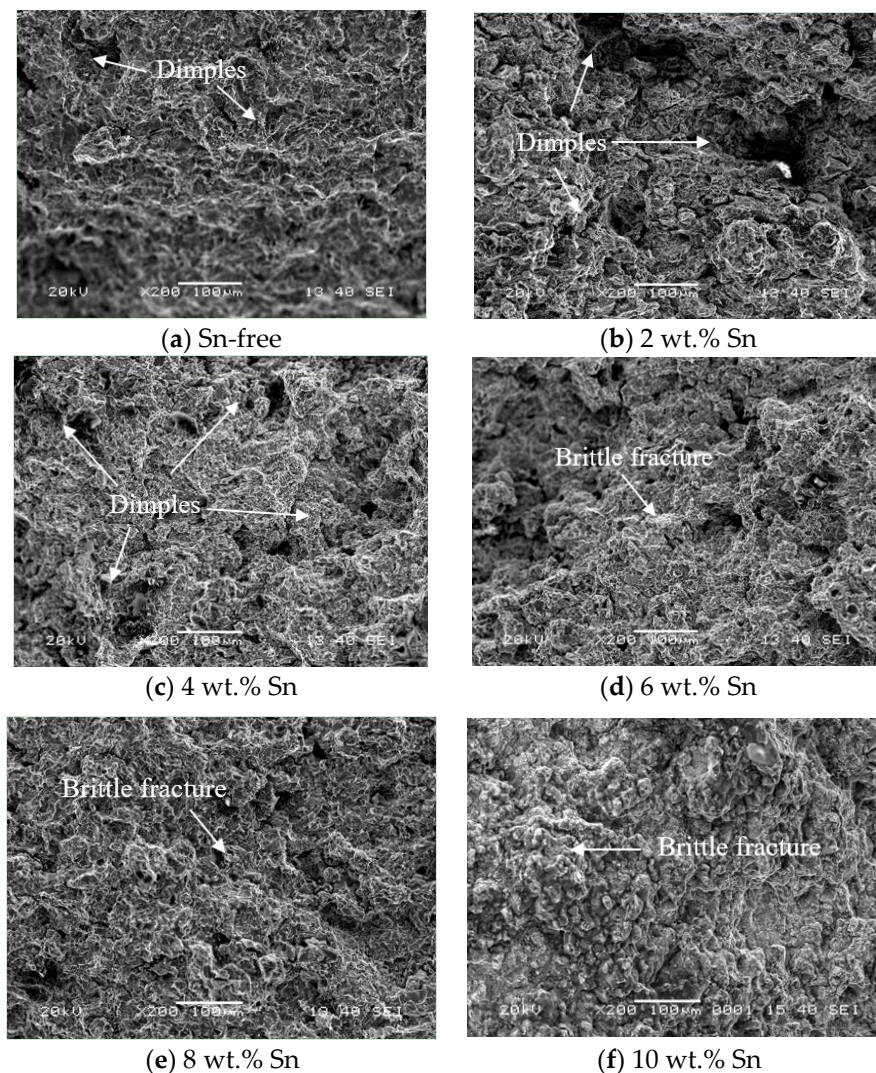


**Figure 8.** SEM fracture of matrix after three-point bending with different Sn contents.

### 3.2.3. Effect of Sn Content on Bending Strength of Cutter Head of Diamond

After adding diamond into the powder, the cutter head is made by mixing, pressing and sintering. Figure 9 shows the effect of Sn content on the bending strength of diamond tools and the holding coefficient of the sintered matrix on diamond. The bending strength increases first and then decreases, and reaches the maximum when the content of Sn reaches 4%. The bending strength of the cutter head is consistent with the bending strength of the blank matrix. However, the bending strength of the cutter head is much lower than that of the blank matrix. Moreover, the effect of Sn on the holding coefficient of sintered matrix to diamond was significant. The holding coefficient is equal to the bending strength of the matrix divided by the bending strength of the diamond cutter head [31]. The value of the holding coefficient is high when the Sn content is 4 wt.%. This indicates that there is good joining performance between the matrix and diamond with 4 wt.% Sn addition.

Figure 10 shows the bending fracture morphologies of diamond tools under pre-alloyed powders with different Sn contents. It can be seen from Figure 10a that the fracture of Sn-free diamond tools contains some big pores, which corresponded to a low holding coefficient of the sintered matrix on the diamond and a low bending strength of diamond tools. When the Sn content of pre-alloyed powders is increased up to 4 wt.%, the number of pores is decreased, the size of the pores is reduced, and the number of dimples is increased. Moreover, there is no obvious crack at the fracture (see Figure 10a–c). The results indicate good joining between the matrix and diamond and demonstrate that the service

lifetime of the diamond tool reaches the optimal value when the Sn content of the pre-alloyed powder is 4 wt.%. When the Sn content exceeds 4 wt.%, cracks show at the fracture and the performance of the joint is deteriorated and thus the corresponding service lifetime of diamond tools is reduced (see Figure 10d–f).

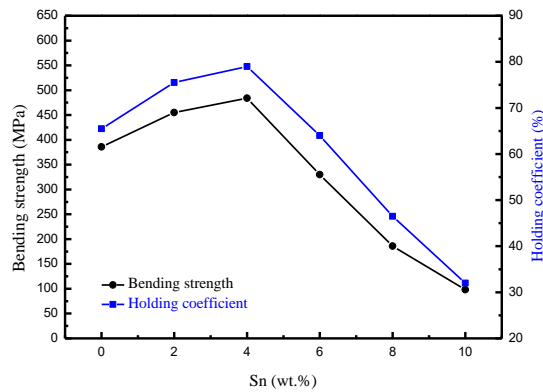


**Figure 9.** The effect of Sn content on the bending strength of diamond tools and holding coefficient of the sintered matrix on diamond.

The EDAX results of the interface between the matrix and the diamond recorded in a point are listed in Table 2. It can be concluded from Table 2 that metallurgical reactions take place between the matrix and diamond with different contents of Sn in pre-alloyed powders. It is well known that Fe has a good wettability on diamond surfaces. Fe reacts with diamonds to form carbides by the diffusion of Fe to the surfaces of diamond, resulting in the increase in holding coefficient of the matrix over the diamond. When the content of Sn in pre-alloyed powders is increased from 0 to 4 wt.%, the content of Sn increases, indicating the good wettability of Cu–Sn as compared to diamond, and the FeC phase is formed. Thus, the diffusion brazed joint is formed and the service life of diamond tools is enhanced. However, when the Sn content is increased from 4 wt.% to 10 wt.%, the amount of liquid phase is increased and some of it flows away, and thus the Cu–Sn brittle phases are formed. Moreover, the formation of cracks between the matrix and diamond is promoted because of the high value of the coefficient of thermal expansion of Sn. Thus, the bending strength of diamond tools is decreased, the holding ability of the matrix on the diamond is decreased and the service life of diamond tools is decreased.

**Table 2.** EDAX results of interface between the matrix and the diamond under pre-alloyed powders with different Sn contents.

Sn Content (wt.%)	Chemical Elements (wt.%)					
	Sn	C	Fe	Cu	Ni	Zn
0	1.91	75.15	15.02	5.69	0.01	2.23
2	2.03	96.12	1.15	0.63	0.07	0
4	2.07	88.56	5.1	3.21	0.08	0.98
6	0	92.64	4.38	1.7	0.58	0.69
8	0.51	92.46	3.04	3.26	0.07	0.65
10	0	78.68	16.84	4.48	0	0

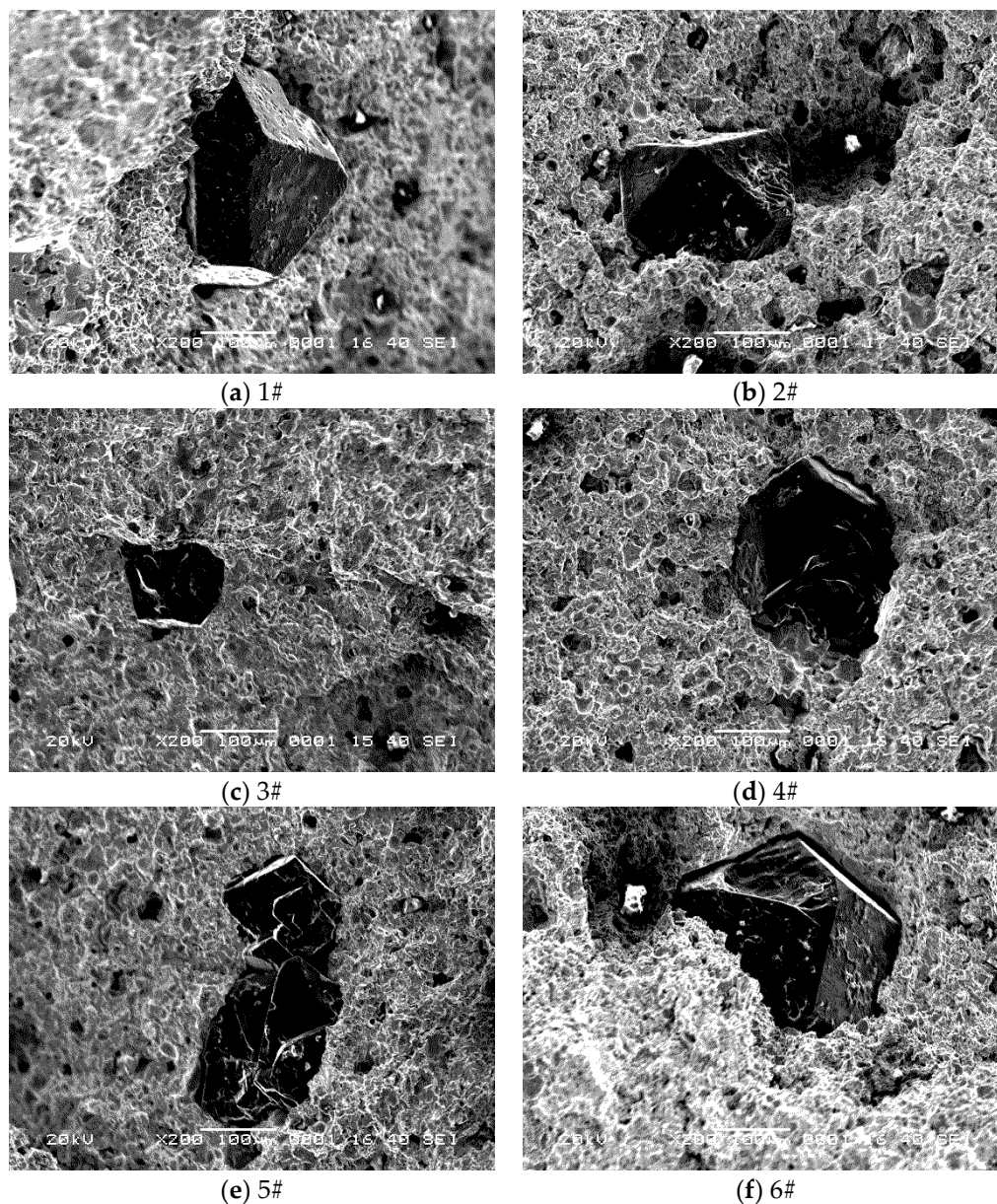


**Figure 10.** The bending fracture morphologies of diamond tools under pre-alloyed powders with different Sn contents.

#### 4. Conclusions

The present work evaluated the microstructure evolution and lifetime extension of Sn added in diamond tools. Accordingly, the following points can be concluded:

- With the increase of Sn content in the experimental pre-alloyed powder, the grain size and the porosity decrease, while the hardness increases. With the increase in Sn content, the microstructure of the matrix becomes more uniform.
- With the increase of Sn content in the pre-alloyed powder up to 4 wt.%, the bending strength of the matrix and the cutter head are both increased firstly, and then decreased when the Sn content exceeds 4 wt.%.
- With the increase of Sn content in the pre-alloyed powder, the fracture morphologies of the matrix changes from a mixed brittle-ductile type of fracture, to ductile fracture, brittle-ductile mixed fracture and brittle fracture.

- The service life of the brazing coating of diamond tools can be greatly prolonged when 4 wt.% Sn content is added in the Fe-based pre-alloyed powder.

**Author Contributions:** Conceptualization, W.L. and M.W.; Methodology, D.L.; Validation, K.Q.; Formal Analysis, J.P.; Investigation, D.L.; Resources, W.L. and M.W.; Data Curation, D.L.; Writing—Original Draft Preparation, D.L.; Writing—Review and Editing, M.W.; Supervision, W.L. and M.W.

**Funding:** This research was funded in part by the Central Plains Scholar Project of Henan Province (172101510003), Funding of China Postdoctoral Science Foundation Funded Project (No. 2016M601753), the Open Project Program of the State Key Laboratory of Advanced Brazing Filler Metals and Technology (SKLABFMT-2017-03) and the Jiangsu Government Scholarship for Overseas Studies (No. JS-2016-133).

**Conflicts of Interest:** The authors declare no conflict of interest.

## References

- Müllen, K.; Antonietti, M. Carbon materials with a kick! *Macromol. Chem. Phys.* **2012**, *213*, 999–1000.
- He, Z.; Katsui, H.; Goto, T. High-hardness diamond composite consolidated by spark plasma sintering. *J. Am. Ceram. Soc.* **2016**, *99*, 1862–1865. [[CrossRef](#)]
- Tönshoff, H.K.; Hillmann-Apmann, H.; Asche, J. Diamond tools in stone and civil engineering industry: Cutting principles, wear and applications. *Diam. Relat. Mater.* **2002**, *11*, 736–741. [[CrossRef](#)]
- Aoqui, S.; Ebihara, K.; Yamagata, Y. Diamond-like carbon film preparation and surface coatings of oxide superconducting and ferroelectric films. *Carbon* **1998**, *36*, 591–594. [[CrossRef](#)]
- Chevallier, E.; Scorsone, E.; Bergonzo, P. Modified diamond nanoparticles as sensitive coatings for chemical SAW sensors. *Procedia Chem.* **2009**, *1*, 943–946. [[CrossRef](#)]
- Das, P.; Paul, S.; Bandyopadhyay, P.P. Plasma sprayed diamond reinforced molybdenum coatings. *J. Alloy. Compd.* **2018**, *767*, 448–455. [[CrossRef](#)]
- Kühl, C.H. Active brazing of diamonds—Technology and application. *Diam. Tool Consult.* **1940**, 1–8.
- Rodríguez-Barrero, S.; Fernández-Larrinoa, J.; Azkona, I.; López de Lacalle, L.N.; Polvorosa, R. Enhanced performance of nanostructured coatings for drilling by droplet elimination. *Mater. Manuf. Process.* **2016**, *31*, 593–602. [[CrossRef](#)]
- Sánchez Egea, A.; Martynenko, V.; Martínez Kraemer, D.; López de Lacalle, L.; Benítez, A.; Genovese, G. On the cutting performance of segmented diamond blades when dry-cutting concrete. *Materials* **2018**, *11*, 264. [[CrossRef](#)] [[PubMed](#)]
- Egea, A.S.; Martynenko, V.; Abate, G.; Deferrari, N.; Kraemer, D.M.; de Lacalle, L.L. Friction capabilities of graphite-based lubricants at room and over 1400 K temperatures. *Int. J. Adv. Manuf. Technol.* **2019**, *102*, 1623–1633. [[CrossRef](#)]
- Johnsen, B.B.; Kinloch, A.J.; Mohammed, R.D.; Taylor, A.C.; Sprenger, S. Toughening mechanisms of nanoparticle-modified epoxy polymers. *Polymer* **2007**, *48*, 530–541. [[CrossRef](#)]
- Zhang, X.; Wang, Y.; Zang, J.; Cheng, X.; Xu, X.; Lu, J. Depression effects of Al on oxidation of diamond during sintering of diamond/borosilicate glass composites. *Int. J. Appl. Ceram. Technol.* **2012**, *9*, 143–148. [[CrossRef](#)]
- Felde, B.; Mehner, A.; Kohlscheen, J.; Gläbe, R.; Hoffmann, F.; Mayr, P. Deposition of alumina coatings on monocrystalline diamonds by sol-gel techniques. *Diam. Relat. Mater.* **2001**, *10*, 515–518. [[CrossRef](#)]
- Thakur, B.N. Examination of technical parameters involved in the metal bond development for diamond impregnated products (a primer for end-users). *Ind. Diam. Rev.* **1977**, 91–93.
- Popov, A.V. Failure of diamond grains at the working surface of grinding wheels. *Russ. Eng. Res.* **2009**, *29*, 838–840. [[CrossRef](#)]
- Henderer, W.; Xu, F. Hybrid TiSiN, CrC/C PVD coatings applied to cutting tools. *Surf. Coat. Technol.* **2013**, *215*, 381–385. [[CrossRef](#)]
- Weimin, L.; Wenming, L.; Kun, Z.; Sujuan, Z.; Wei, Z.; Wei, L.; Jintao, Z. Brazing effects of pre-alloyed powder in sintering of diamond tool. *Weld. Join.* **2008**, *3*.
- Zhao, X.; Duan, L.; Chikhotkin, V.F.; Weng, H. Summary on holding force of metallic matrix to diamond. *Diam. Abras. Eng.* **2015**, *6*, 41–46.
- Long, W.M.; Liu, W.M.; Zhu, K.; Zhong, S.J.; Zou, W.; Li, W.; Zhao, J.T. Brazing connection of cash diamond by prebonding technology. *Weld. Join.* **2008**, *3*, 14–17. (In Chinese)

20. Zhong, S.J.; Long, W.M.; Cheng, Y.F. Brazing technology of effectively improve diamond tools life and cutting efficiency. *Mater. Sci. Technol.* **2009**, *1*, 222–225.
21. Sazanov, Y.N. Applied significance of polyimides. *Russ. J. Appl. Chem.* **2001**, *74*, 1253–1269. [[CrossRef](#)]
22. Zhou, Y.M.; Lv, Z.; Zhang, J.Z.; Chen, G.X. Application of brazing technology in diamond tools. *Tool Eng.* **2004**, *3*, 9–12.
23. Xu, Q.; Liu, Y.B.; Xu, L.; Yang, Z.W. Properties of Fe-based pre-alloy powders with different contents. *Powder Metall. Technol.* **2017**, *2*, 24–28. (In Chinese)
24. Nasrabadi, H.Y.; Salahi, E.; Taati Asil, F. Evaluation of dynamic viscosity and rheological properties of ceramic materials during liquid phase sintering by numerical-experimental procedure. *Int. J. Appl. Ceram. Technol.* **2017**, *14*, 1222–1235. [[CrossRef](#)]
25. Zhai, Q.Y.; Yang, Y.; Xu, J.F.; Guo, X.F. Microstructural morphology and phase structure of rapidly solidified Cu-Sn alloy. *Chin. J. Nonferrous Met.* **2006**, *16*, 1374–1379.
26. Qin, H.Q.; Lu, A.J.; Lin, F.; Meng, G.H.; Cheng, Y. Research of free sintering process of diamond tool matrix. *Superhard Mater. Eng.* **2016**, *28*, 6–9.
27. Ding, H.D.; Li, Y.W.; Hao, H.Q.; Jin, Z.H. Decreasing the sintering temperature of diamond-bit matrix material by the addition of the element P. *J. Mater. Process. Technol.* **1998**, *74*, 52–55. [[CrossRef](#)]
28. Meng, G.; Lei, X.; Lu, A.; Qin, H.; Lin, F. Effects of CuSn<sub>15</sub> and Fe on the properties of pressureless sintered diamond tools matrix. *Powder Metall. Technol.* **2015**, *33*, 105–110.
29. Xu, J.J.; Wan, L.; Song, D.D.; Wang, J.S.; Liu, Y.Y. Influence of Cu content on the properties of the Al-based binding agent and diamond tool. *Mater. Rev.* **2017**, *31*, 104–108.
30. Ding, T.; Long, W.; Qiao, P.; Pei, Y. Effect and mechanism of pre-alloy powder on microstructure of diamond composite. *Trans. China Weld. Inst.* **2011**, *32*, 75–78.
31. Lu, A.J.; Qing, H.Q.; Lei, X.X.; Meng, G.H.; Lin, F.; Cheng, Y. Effect of Ni on matrix properties of free sintered diamond tools. *Superhard Mater. Eng.* **2004**, *2*, 35–38. (In Chinese)



© 2019 by the authors. Licensee MDPI, Basel, Switzerland. This article is an open access article distributed under the terms and conditions of the Creative Commons Attribution (CC BY) license (<http://creativecommons.org/licenses/by/4.0/>).